



ELSEVIER

Radiotherapy and Oncology 69 (2003) 251–258

RADIOTHERAPY
& ONCOLOGY
JOURNAL OF THE EUROPEAN SOCIETY FOR
THERAPEUTIC RADIOLOGY AND ONCOLOGY

www.elsevier.com/locate/radonline

A comparison of forward and inverse treatment planning for intensity-modulated radiotherapy of head and neck cancer

Werner Bär^a, Marco Schwarz^b, Markus Alber^{a,*}, Luc J. Bos^b, Ben J. Mijnheer^b,
Coen Rasch^b, Christoph Schneider^b, Fridtjof Nüsslin^a, Eugene M.F. Damen^b

^aMedical Physics Division, University Hospital for Radiation Oncology, Hoppe-Seyler-Str. 3, Tübingen 72076, Germany

^bDepartment of Radiotherapy, The Netherlands Cancer Institute/Antoni van Leeuwenhoek Hospital, Plesmanlaan 121, Amsterdam 1066 CX, The Netherlands

Received 4 November 2002; received in revised form 8 August 2003; accepted 13 August 2003

Abstract

Background and purpose: To compare intensity-modulated treatment plans of patients with head and neck cancer generated by forward and inverse planning.

Materials and methods: Ten intensity-modulated treatment plans, planned and treated with a step&shoot technique using a forward planning approach, were retrospectively re-planned with an inverse planning algorithm. For this purpose, two strategies were applied. First, inverse planning was performed with the same beam directions as forward planning. In addition, nine equidistant, coplanar incidences were used. The main objective of the optimisation process was the sparing of the parotid glands beside an adequate treatment of the planning target volume (PTV). Inverse planning was performed both with pencil beam and Monte Carlo dose computation to investigate the influence of dose computation on the result of the optimisation.

Results: In most cases, both inverse planning strategies managed to improve the treatment plans distinctly due to a better target coverage, a better sparing of the parotid glands or both. A reduction of the mean dose by 3–11 Gy for at least one of the parotid glands could be achieved for most of the patients. For three patients, inverse planning allowed to spare a parotid gland that had to be sacrificed by forward planning. Inverse planning increased the number of segments compared to forward planning by a factor of about 3; from 9–15 to 27–46. No significant differences for PTV and parotid glands between both inverse planning approaches were found. Also, the use of Monte Carlo instead of pencil beam dose computation did not influence the results significantly.

Conclusion: The results demonstrate the potential of inverse planning to improve intensity-modulated treatment plans for head and neck cases compared to forward planning while retaining clinical utility in terms of treatment time and quality assurance.

© 2003 Elsevier Ireland Ltd. All rights reserved.

Keywords: Intensity-modulated radiotherapy; Step&shoot; Forward planning; Inverse planning; Head and neck cancer

1. Introduction

Previous comparisons between conventional and intensity-modulated treatment planning have demonstrated the potential to improve dose distributions with intensity-modulated radiotherapy (IMRT) for several tumour sites [21]. IMRT can be delivered in a static mode, where a series of single fields or segments from each beam direction are superimposed to achieve a modulation of the intensity [6]. In this paper, we will denote this method as the step&shoot technique. Two approaches of computerised treatment planning for step&shoot IMRT are generally applied:

the first method is an extension of conventional treatment planning and is in this paper referred to as forward planning. Its definition of the segment shapes is performed manually similar to conventional planning. However, more than one segment is used from each beam direction. Afterwards, the weights of the segments are optimised using a computer optimisation algorithm to achieve the desired dose distribution [9,10–12,20]. The second strategy, which we denote as inverse planning, usually starts with the optimisation of fluence profiles from each beam direction by minimisation of an objective function [5,7]. Afterwards, sequencing transforms each optimised profile into a series of segments, which can be delivered with a multileaf collimator (MLC).

* Corresponding author.

Alternatively, sequencing may also be part of the optimisation process [3,23,30].

The clinical implementation of IMRT using forward planning is relatively easy, because it is closely related to conventional planning. Issues like quality assurance, time involved in planning and delivery are a logical extension of the experience obtained with conformal radiotherapy. Manual definition of the segments leads to intuitive choices of the segment shapes based on the beam's eye view option of the planning system. Inverse planning is far less related to conventional radiotherapy because the segment shapes are not defined manually and the number of segments is usually considerably larger. However, there are complex clinical situations, which require the use of many beam directions and segments. In these cases, inverse planning may be the more efficient strategy.

The aim of this work was to investigate if, and to what degree, improvements of IMRT treatment plans generated by forward planning can be achieved with an inverse planning strategy for complex treatments. To this aim, we compared a clinically applied forward planning procedure with an inverse planning technique for a set of patients suffering from head and neck tumours. IMRT for these tumour sites is considered to be a promising method to improve local control and/or reduce acute or late toxicity [25,32]. In particular, the aim of the treatment planning was to spare the parotid glands to avoid or alleviate xerostomia without compromising the coverage of the planning target volume (PTV). This approach is based on considerations and results of recent publications from the University of Michigan [13–15] and other institutions [8,28,32–34].

2. Methods and materials

Ten patients with various types of head and neck cancer were selected for this planning study (tumour sites: base of tongue: 7, tumour volume 323–748 cm³, median 530 cm³; larynx: 3, tumour volume 363–503 cm³, median 424 cm³). All patients received a CT-scan with a slice distance of 3 mm. Treatment planning and delivery were performed at the Netherlands Cancer Institute (NKI) between October 2000 and January 2002 with the forward planning approach described in Section 2.1. All patients were treated with 6 MV photons produced by Elekta SL 15 accelerators. In two cases, an additional electron boost was delivered to treat regions in very close proximity to the patient surface.

The PTV of the main phase of the treatment, further denoted as PTV1, consisted of the primary tumour and the left and right nodes, with a safety margin to account for organ motion and set-up variations. Although PTV1 consisted of three separate volumes in some cases, in what follows, we refer to PTV1 as one composite volume. For both planning methods, the PTV1 was slightly modified to keep a minimum distance of 5 mm to the patient surface. In this way, the build-up region, where it is impossible to meet

the prescribed target coverage and where the dose calculation is imprecise, was excluded. After the optimisation, the segments produced by the inverse planning procedure were enlarged to cover the volume of PTV1 close to the patient surface. The spinal cord and both parotid glands were considered as organs at risk (OARs).

A dose of 46 Gy was prescribed to the ICRU point at the centre of the primary tumour for the main phase of the treatment. Patients were treated 5 times per week with a total dose of 46 Gy given in 23 fractions. Subsequently, a boost of typically 24 Gy was delivered with the same fractionation scheme to PTV2, which consisted of the high risk volumes of PTV1 and to parts of the neck nodes where indicated.

The aims of the treatment were to achieve a dose of 90% of the prescribed dose (46 Gy for the main phase, 24 Gy for the boost) in at least 99% of the volume of PTV1 and PTV2 and a dose of 95% in at least 97% of PTV1 and PTV2. The maximum dose was restricted to 107% of the prescribed dose in each treatment phase. The maximum dose of the spinal cord was limited to 50 Gy for the composite treatment plan. Furthermore, the mean dose of either parotid gland should not exceed 26 Gy for the composite treatment. This limitation aims at sparing the gland function according to the findings of Eisbruch et al. [15]. However, not all aims of the planning could be achieved for each patient due to the geometry of PTV1, PTV2 and OARs in these patients (see Section 3.1).

2.1. Forward treatment planning

Forward treatment planning of the main phase was performed with the 3D treatment planning system U-MPLAN (University of Michigan [18]), which is used in clinical routine at the NKI. The first planning stage consisted of manually specifying 5–10 beam incidences for each patient which are suitable to irradiate PTV1 properly while having the potential to spare the OARs. Segments were manually defined, typically either encompassing PTV1 completely or partially, while shielding the OARs. The total number was limited to 20 segments. U-MPLAN uses an edge/octree dose computation algorithm [19,26]. In the next step, an optimisation of the beam weights was performed for all segments with a module of the treatment planning system [17]. The cost functions for the optimisation reflected the aims of the treatment planning. Their general usage is described in detail elsewhere [29]. For this study, the aforementioned aims for PTV1 and a maximum dose of 40 Gy to the spinal cord were chosen for the main phase. Another aim of this phase was to restrict the volume of each parotid gland that receives more than 25 Gy to 60% of the total volume. If a parotid gland could not be spared, i.e. if this aim could not be reached, this gland was removed from the optimisation. After the optimisation, segments with less than 4 monitor units (MU) were eliminated and the optimisation was

restarted with the remaining segments. This procedure was repeated until all segments delivered at least 4 MU.

A similar but less complex method was applied for the boost phase, where only 2–4 beam incidences were used. Furthermore, beam weight optimisation was considered to be unnecessary due to the rather simple design of the treatment plans of the boost.

2.2. Inverse treatment planning

Inverse treatment planning was performed with the inverse planning software HYPERION (University of Tübingen [1,2]). Briefly, HYPERION minimises the probability of tumour cell survival subject to constraints for the PTVs and OARs. The optimisation considers the constraints in a strict way and not through the use of importance factors. Violations of the prescription are only accepted for PTV1, but not for the OARs. In an initial stage of the optimisation, HYPERION uses a finite-size pencil beam algorithm with density scaling to produce freely modulated fluence weight profiles. In a second stage, the shapes and weights of segments are optimised. Here, the Monte Carlo code XVMC can be used [16,24] alternatively.

In the beginning of the planning procedure of the main phase, beam directions and cost functions that reflect the desired dose distribution were specified. In a first series of optimisation (1st inverse approach), the same beam directions as applied for the specific patient during forward planning were defined. In a second series (2nd inverse approach), nine equidistant and coplanar beam directions starting from 0° gantry angle were used.

A class solution for the cost functions was defined (See Appendix A for details). For PTV1, the aim was to minimise the probability of tumour cell survival with a Poisson statistical model. Additionally, a dose variance constraint was used to control the steepness of the cumulative dose volume histogram (DVH) of PTV1. An overdose constraint contributed a penalty to the objective function if the prescribed dose of 46 Gy was exceeded. A serial constraint for the spinal cord limited its maximum dose to the same value as achieved with forward planning. A parallel constraint was used for either parotid glands to control the mean dose. The aim for the main phase was to achieve a mean dose of not more than 20 Gy for each parotid gland. The parotid constraints used for inverse planning are somewhat stricter than for forward planning in order to force better sparing. If this resulted in an unacceptable coverage of PTV1, the constraints were modified to allow a higher mean dose. Note that a step like this has to be taken because otherwise, inverse planning would create less modulated treatment plans quite like forward planning. Better parotid sparing will not result from the use of inverse planning alone unless it is required in the treatment setup. As before, a parotid gland that could not be spared was ignored as a dose-limiting organ. An overdose constraint with a much lower tolerance than for PTV1 was used for

the remaining patient volume to suppress hot spots outside PTV1.

At first, the fluence profiles were optimised. Subsequently, each profile was transformed into an initial series of segments. Finally, the shapes and weights of the resulting segments were re-optimised with the same cost functions as used for initial fluence optimisation. Additional constraints were applied to force the optimisation to produce reasonably shaped segments. The minimum segment size was limited to 4 cm², the minimum segment width to 1 cm and the minimum segment weight to 5 MU. A detailed description of this automated procedure, which did not require user intervention at intermediate stages, can be found elsewhere [3,4].

The planning of the boost phase was performed with a single approach with similar cost functions. In some cases, the same beam directions as for forward planning were used. In others, different incidences were specified to be able to reduce the dose to the parotid glands compared to forward planning.

For the comparison of the treatment plans, the DVHs were normalised, so that the mean dose of PTV1 of the primary tumour was equal to 46 Gy for the main phase and the mean dose of PTV2 was equal to 24 Gy for the boost. We analysed the coverage of PTV1 and PTV2, the maximum dose of the spinal cord and the mean doses of both parotid glands. We did not consider the maximum dose of PTV1 and PTV2 in what follows, because they were in every case similar for all methods.

3. Results

3.1. Main phase

Forward treatment planning of the main phase resulted in 5–10 beams and 9–15 segments. The 1st inverse planning approach with the same beam directions led to 27–42 segments, while the 2nd with nine equidistant beams resulted in 24–46 segments (Table 1).

The aim of having at least 99% of the volume of PTV1 to receive at least 90% of the prescribed dose was in most cases fulfilled for all three approaches. Only forward planning of patient 6 led to significant underdosage. The criterion of having at least 97% of PTV1 to receive at least 95% of the prescribed dose was mostly not met by any method (on an average 86.9% of the volume of PTV1 for forward planning, 95.5% for 1st inverse and 95.4% for 2nd inverse planning received 95% of the prescribed dose), although the extent of failure varied significantly (68–97% for forward planning, 92–98% for 1st inverse and 93–98% for 2nd inverse planning). The maximum dose to the spinal cord was in most cases similar (on an average 40.8 Gy for forward, 39.4 Gy for 1st inverse and 39.5 Gy for 2nd inverse planning). Only for patient 4, one of the inverse approaches exceeded the result of the forward technique. For three

Table 1
Results of the three treatment planning techniques for the main phase

		Patient									
		1	2	3	4	5	6	7	8	9	10
%Volume of PTV1 receiving 90% of 46 Gy	Forward	100	98	98	99	100	95	100	99	100	98
	1st Inverse	98	99	99	100	99	98	100	99	99	99
	2nd Inverse	99	99	99	99	99	98	100	100	99	99
%Volume of PTV1 receiving 95% of 46 Gy	Forward	94	83	91	91	92	68	97	85	96	72
	1st Inverse	95	95	96	96	96	92	98	96	96	95
	2nd Inverse	95	97	95	93	95	94	98	96	96	95
Maximum dose (Gy) of the spinal cord	Forward	40	40	41	41	40	41	41	41	45	38
	1st Inverse	39	39	40	41	38	41	40	39	42	35
	2nd Inverse	38	40	41	43	39	41	40	38	41	34
Mean dose (Gy) of the left parotid gland	Forward	30	28	–	19	27	23	26	14	25	26
	1st Inverse	19	23	–	20	19	19	18	13	21	21
	2nd Inverse	19	24	–	20	20	17	19	15	22	20
Mean dose (Gy) of the right parotid gland	Forward	23	–	24	18	24	23	16	15	24	–
	1st Inverse	19	–	20	20	19	22	17	12	20	–
	2nd Inverse	19	–	19	22	19	20	19	11	21	–
#Beams	Forward	6	6	9	5	7	8	6	6	10	7
	1st Inverse	6	6	9	5	7	8	6	6	10	7
	2nd Inverse	9	9	9	9	9	9	9	9	9	9
#Segments	Forward	9	10	11	11	11	12	12	12	15	13
	1st Inverse	38	37	30	27	28	29	33	39	42	41
	2nd Inverse	35	32	27	24	30	46	30	31	33	39

'Forward' displays the results of the clinically applied forward planning technique, '1st Inverse' of the inverse planning technique with the same beam directions and '2nd Inverse' of the inverse planning technique with nine equidistant beams. The entries for three parotid glands which had to be sacrificed by all techniques are marked by –. The forward and 1st inverse plans used the same beam directions, while the 2nd inverse plan consisted of nine equispaced coplanar beams.

patients, none of the methods managed to spare both parotid glands (patients 2, 3 and 10). Most of the time, both inverse planning methods resulted in 3–11 Gy lower doses to at least one of the parotid glands. Only for patients 4 and 7, the mean dose of the right parotid gland was somewhat higher with the 2nd inverse approach compared to that of the forward planning. Both inverse planning approaches led to similar results in terms of coverage of PTV1 and sparing of OARs. The results for the three approaches are summarised in Table 1 for all 10 patients. As a typical example, the results of forward and 1st inverse planning of patient 5 for PTV1 of the primary tumour and the parotid glands are illustrated in a cumulative DVH in Fig. 1.

3.2. Boost phase

Forward treatment planning of the boost phase resulted in 2–4 beams and 2–5 segments. Inverse planning applied 3–4 directions and resulted in 8–26 segments. The complexity of inverse planning significantly increased if it was possible to spare an additional parotid gland (Table 2). For instance, the number of segments increased from 4 to 26 for patient 5. Inverse planning was not performed for patients 9 and 10, who received a boost treatment with electrons. The differences with respect to coverage of PTV2 were small and no method was systematically better than another. The maximum dose of the spinal cord was similar or lower for the inverse planning approach. We achieved

significantly lower mean doses for one of the parotid glands for patients 1, 5 and 7 with inverse planning, while the results were similar in the other cases.

3.3. Composite treatment

Since the results for PTV1 and PTV2 were already sufficiently analysed in the previous sections, this section is focussed on the total mean dose of the parotid glands. For the sake of simplicity, we consider only the forward

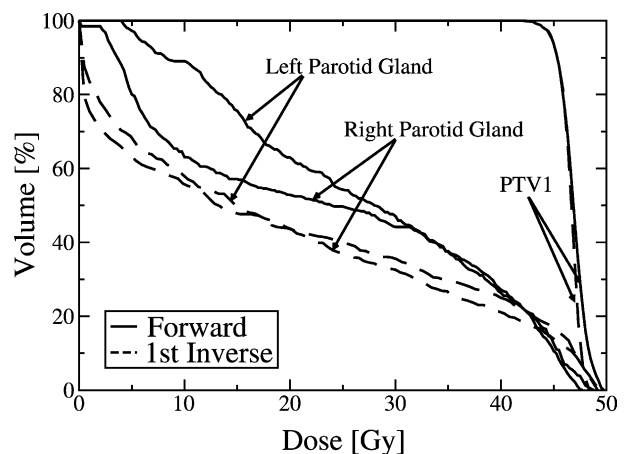


Fig. 1. Cumulative DVH of PTV1 of the primary tumour and the parotid glands of forward and 1st inverse plan of patient 5.

Table 2
Results of forward and inverse planning of the boost phase

		Patient							
		1	2	3	4	5	6	7	8
%Volume of PTV2 receiving 90% of 24 Gy	Forward	100	100	93	100	100	100	99	91
	Inverse	98	99	97	99	99	100	99	100
%Volume of PTV2 receiving 95% of 24 Gy	Forward	98	97	90	95	98	100	97	89
	Inverse	96	95	94	96	95	99	97	98
Maximum dose (Gy) of the spinal cord	Forward	10	9	7	7	12	10	10	4
	Inverse	8	9	6	5	11	10	7	4
Mean dose (Gy) of the left parotid gland	Forward	14	1	–	2	10	3	13	2
	Inverse	7	0	–	1	4	0	8	0
Mean dose (Gy) of the right parotid gland	Forward	0	–	0	2	1	1	2	–
	Inverse	0	–	1	1	1	0	1	–
#Beams	Forward	3	3	3	3	4	3	3	2
	Inverse	4	3	4	3	4	3	4	4
#Segments	Forward	5	4	3	3	4	3	4	2
	Inverse	14	12	20	10	26	8	20	18

and the 1st inverse planning approach, where the same beam directions were used.

For three patients, inverse planning managed to save a parotid gland, which could not be spared with forward planning (patients 1, 5 and 7). In three other cases, both methods had to sacrifice a parotid gland (patients 2, 3, and 10). In the rest of the cases, inverse planning resulted on average in lower mean doses. In Fig. 2, the mean dose of the composite treatment of one of the parotid glands of each patient are illustrated in a histogram for the forward and the 1st inverse planning approach. For patients 9 and 10, where the boost was not planned with HYPERION, we used results of the main phase only. In Fig. 3, the results for the parotid glands of forward and 1st inverse planning are illustrated in a different way: the amount of parotid glands given as a percentage of the total number (9 left and 8 right parotid glands, as we did not consider the three parotid glands that were sacrificed by all approaches) that received equal or more dose than the specified is plotted against the dose. This plot shows a distinct shift of the mean dose in the parotid

glands towards lower values for the inverse compared to the forward approach.

4. Discussion

The results of our study showed distinctly improved dose distributions for treatment of head and neck cancer for inverse planning compared to forward planning. These improvements either concerned the coverage of PTV1 (patients 2, 6, 8 and 10) or the sparing of the parotid glands (patients 1, 5 and 7). On the other hand, inverse planning increased the number of segments compared to forward planning distinctly (about the threefold for the main phase) and thus decreased the average weight of a segment. However, the treatment time with modern step&shoot delivery methods is mainly determined by the number of gantry angles, at least when the number of segments is less than 30–40. Treatments with step&shoot IMRT with that many segments are thus not significantly prolonged

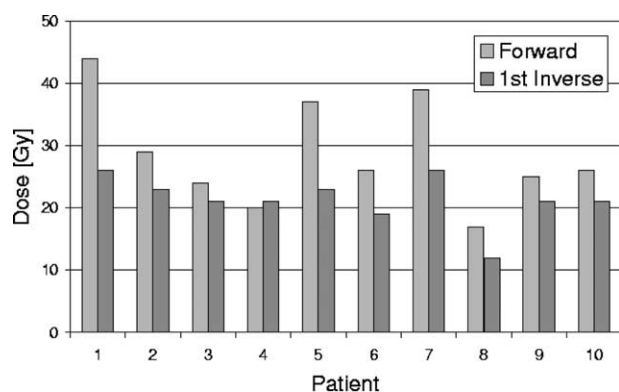


Fig. 2. Histogram of the results for the mean dose of the parotid glands for all 10 patients after forward and inverse planning of both treatment phases. For each patient, the parotid gland with the larger difference between both methods was chosen for this illustration (see Tables 1 and 2 for details).

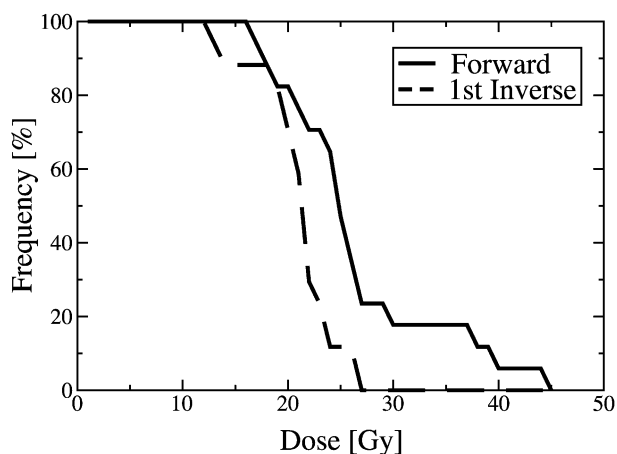


Fig. 3. Frequency of the total number of parotid glands that received equal or less dose than the specified dose.

compared to conventional therapy. Similar to forward planning, inverse planning limited the minimum weight of any segment to 5 MU.

In our study, the major aim for the parotid glands was to achieve a mean dose below 26 Gy as proposed by Eisbruch et al. [15]. We considered a mean dose of 26 Gy as sufficient to substantially spare the gland function. However, the normal tissue complication probability (NTCP) for the parotid glands published by Eisbruch et al. [15] and another group [28] are continuous and monotonously increasing functions of the mean dose with a steep gradient between 20 and 30 Gy. Any significant reduction of the mean dose in this range may thus be of clinical importance. Therefore, the benefits of inverse planning with respect to the parotid glands may not only be relevant for patients 1, 5 and 7, but also for patients 2, 3, 6, 9 and 10.

The comparison of the 1st and the 2nd inverse planning strategy did not show distinctly different results. The 1st approach with on average fewer and manually chosen beam directions was more efficient with respect to the delivery time, while the 2nd strategy with nine equally spaced beam directions was faster and easier to plan. These results support the hypothesis that IMRT with equidistant, coplanar beams, as for instance proposed by Stein et al. [31] for prostate cancer, may not always be optimal for treatment of head and neck cases. For these tumours, automated beam direction optimisation seems more promising [27].

The validity of this study could be compromised by the fact that the two strategies employ different dose computation algorithms. It is important to distinguish between the absolute accuracy of a dose computation method, as compared with measurement, and the influence of inaccuracies on the results of an optimisation algorithm. Regarding the former point, recomputing the final dose distributions with a third algorithm would only highlight the differences of the respective dose computation methods without giving any insight into the interaction between dose computation and optimisation. Regarding the latter point, if a better dose computation algorithm was used for optimisation, a *different* solution would be produced, which would not need to be *better* with respect to the cost function. These sources of error have been termed ‘systematic’ and ‘convergence’ error in a recent publication by Jeraj et al. [22].

To evaluate the magnitude of the convergence error, the same dose computation method would have to be used *within* the optimisation, which was not possible. However, the optimisation of segment shapes and weights of the inverse algorithm can use either pencil beam or Monte Carlo dose computation. In order to assess the magnitude of the convergence error, a number of cases were optimised again using Monte Carlo. Note, that since the inverse approach employs constrained optimisation, both results will necessarily agree in the OAR and PTV constraints. Hence, the discrepancy between the dose computation algorithms will only affect the cost function of the PTV.

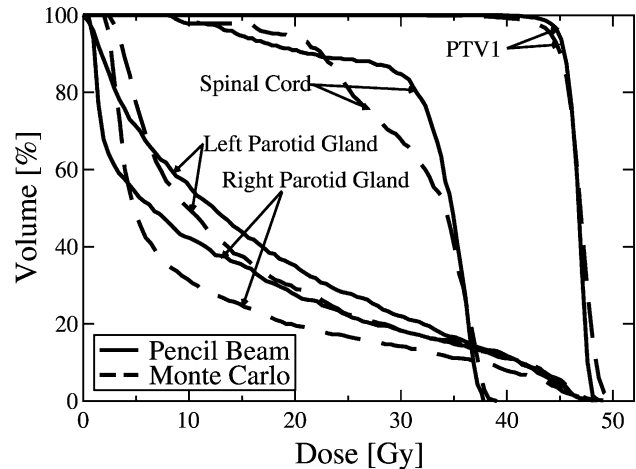


Fig. 4. Cumulative DVH of the dose distribution resulting from the inverse planning of patient 7 with a pencil beam and a Monte Carlo dose calculation algorithm. Illustrated are PTV1, spinal cord and parotid glands.

As an example, we present a very complex case (patient 7), see Fig. 4. The resulting weights and shapes of the segments were slightly different. Note that the segment shapes can be changed in increments of 2 mm in leaf direction, so that any difference in field penumbra between dose computation methods can be easily absorbed in the segment shapes. The largest differences were found in regions that do not affect the value of the cost function (e.g. build-up regions and boundaries of the lung). Although the DVHs of the parotids differ between the pencil beam and Monte Carlo results, their cost function value is equivalent. Compared with pencil beam, a larger volume of the parotids receives low doses with Monte Carlo dose computation, which is due to a better model of accelerator head scatter. Since the parotid dose is constrained by a parallel model, which penalizes also low and intermediate doses, the optimisation algorithm has to compensate for this difference in dose computation. It does so by reducing the volume of the parotids that receives intermediate doses, because this incurs a smaller cost in terms of target coverage than reducing high dose volumes close to the targets. Despite this redistribution of dose in the parotids, the target dose did not suffer significant losses.

These findings imply that the final cost function of the inverse strategy depends weakly on the absolute accuracy of the dose computation, while the segment shapes and weights naturally have a greater dependence. It appears reasonable to assume that these findings could be repeated if the dose computation of the forward strategy could be used within the inverse optimisation so that the differences in dose computation do not bear on the results of this study.

5. Conclusions

A treatment planning comparison of forward and inverse planning for head and neck cancer was performed

in 10 patients. In most of these patients, distinctly better sparing of the parotid glands could be achieved with inverse planning without compromising the coverage of the PTVs. This result is in agreement with other publications regarding forward optimisation strategies for head and neck cancer [20]. However, it was shown by De Gersem et al. [10,11] that the dose distribution can be improved further if the shapes of the segments are adapted during the optimisation, which in effect raises the degrees of freedom of the setup to the levels of inverse planning. Accordingly, our results demonstrate that inverse planning has the potential to improve dose distributions significantly at the cost of a higher number of field segments.

Acknowledgements

We are indebted to Emmy Lamers for her help with generating the clinically applied forward treatment plans. W.B. was supported by grants of the Deutsche Krebshilfe e.V. and the Fortüne-program. M.S. and L.B. were financially supported by The Dutch Cancer Society (NKB Grant NKI 2000-2212). M.A. was supported by DFG Grant NU 33/7-1.

Appendix A

Inverse treatment planning with HYPERION used the following types of objectives and constraints for the definition of cost functions

$$\text{Poisson : } \frac{1}{n} \sum_{i=1}^n \exp(-D_i)$$

$$\text{Overdose : } \frac{1}{n} \sum_{i=1}^n \left(\frac{D_i - D_0}{I} \right)^2 \Theta(D_i - D_0) \leq 1$$

$$\text{Variance : } \frac{1}{n} \sum_{i=1}^n \left(\frac{D_i - \bar{D}}{I} \right)^2 \leq 1$$

$$\text{Serial : } \frac{1}{n} \sum_{i=1}^n \left(\frac{D_i}{I} \right)^k \leq 1$$

$$\text{Parallel : } \frac{1}{n} \sum_{i=1}^n \frac{I}{1 + \left(\frac{D_0}{D_i} \right)^k} \leq 1$$

where n is the number of voxels per structure, D_i the dose in voxel i , \bar{D} the mean dose, $\Theta(x)$ the step function and D_0 , I and k are user-defined parameters. The settings for the main phase were as follows. For PTV1, a Poisson objective, an overdose constraint with $D_0 = 46$ Gy and $I = 1$ Gy, and a variance constraint with $I = 1.5$ Gy was used. A serial constraint with $k = 15$ and $I = 30$ –40 Gy (for most patients $I = 33$ Gy) was applied for the spinal cord. A parallel constraint with $k = 1$ and $D_0 = 16$ –20 Gy was

used for the parotid glands. A lower value for D_0 was applied for the simpler cases, a higher value for difficult cases. Finally, an overdose constraint with $D_0 = 46$ Gy and $I = 0.1$ Gy was used for the remaining volume of the patient excluding PTV1 and OARs. A similar, but down-scaled scheme was used for the boost phase.

References

- [1] Alber M, Birkner M, Laub W, Nüsslin F. Hyperion—an integrated IMRT planning tool. In: Proceedings of 13th International Conference on the Use of Computers in Radiation Therapy. Heidelberg: Springer; 2000. p. 46–8.
- [2] Alber M, Nüsslin F. An objective function for radiation treatment optimization based on local biological measures. *Phys Med Biol* 1999; 44:479–93.
- [3] Alber M, Nüsslin F. Optimization of intensity modulated radiotherapy under constraints for static and dynamic MLC delivery. *Phys Med Biol* 2001;46:3229–39.
- [4] Bär W, Alber M, Nüsslin F. A variable fluence step clustering and segmentation algorithm for step and shoot IMRT. *Phys Med Biol* 2001;46:1997–2007.
- [5] Bortfeld T. Optimized planning using physical objectives and constraints. *Semin Radiat Oncol* 1999;9:20–34.
- [6] Bortfeld TR, Kahler DL, Waldron TJ, Boyer AL. X-ray field compensation with multileaf collimators. *Int J Radiat Oncol Biol Phys* 1994;28:723–30.
- [7] Brahme A. Optimized radiation therapy based on radiobiological objectives. *Semin Radiat Oncol* 1999;9:35–47.
- [8] Chao KSC, Deasy JO, Markman J, et al. A prospective study of salivary function sparing in patients with head-and-neck cancers receiving intensity-modulated or three-dimensional radiation therapy: initial results. *Int J Radiat Oncol Biol Phys* 2001;49:907–16.
- [9] Damen EMF, Brugmans MJP, van der Horst A, et al. Planning computer optimization and dosimetric verification of a segmented irradiation technique for prostate cancer. *Int J Radiat Oncol Biol Phys* 2001;49:1183–95.
- [10] De Gersem W, Claus F, De Wagter C, De Neve W. An anatomy-based beam segmentation tool for intensity-modulated radiation therapy and its application to head-and-neck cancer. *Int J Radiat Oncol Biol Phys* 2001;51:849–59.
- [11] De Gersem W, Claus F, De Wagter C, Van Duyse B, De Neve W. Leaf position optimization for step-and-shoot IMRT. *Int J Radiat Oncol Biol Phys* 2001;51:1371–88.
- [12] De Neve W, De Gersem W, Derycke S, et al. Clinical delivery of intensity modulated conformal radiotherapy for relapsed or second-primary head and neck cancer using a multileaf collimator with dynamic control. *Radiother Oncol* 1999;50:301–14.
- [13] Eisbruch A, Kim HN, Terrell JE, Marsh LH, Dawson LA, Ship JA. Xerostomia and its predictors following parotid-sparing irradiation of head-and-neck cancer. *Int J Radiat Oncol Biol Phys* 2001;50: 695–704.
- [14] Eisbruch A, Marsh LH, Martel MK, et al. Comprehensive irradiation of head and neck cancer using conformal multisegmental fields: assessment of target coverage and noninvolved tissue sparing. *Int J Radiat Oncol Biol Phys* 1998;41:559–68.
- [15] Eisbruch A, Ten Haken RK, Kim HM, Marsh LH, Ship JA. Dose volume and function relationships in parotid salivary glands following conformal and intensity-modulated irradiation of head and neck cancer. *Int J Radiat Oncol Biol Phys* 1999;45:577–87.
- [16] Fippel M, Laub W, Huber B, Nüsslin F. Experimental investigation of a fast Monte Carlo photon beam dose calculation algorithm. *Phys Med Biol* 1999;44:3039–54.

- [17] Fraass BA, Kessler ML, McShan DL, et al. Optimization and clinical use of multisegment intensity-modulated radiation therapy for high-dose conformal therapy. *Semin Radiat Oncol* 1999;9:60–77.
- [18] Fraass BA, McShan DL. 3-D treatment planning: I. Overview of a clinical planning system. In: *Proceedings of Ninth International Conference on the Use of Computers in Radiation Therapy*. Amsterdam: North-Holland; 1987. p. 273–6.
- [19] Fraass BA, McShan DL, TenHaken RK, Hutchins KM. 3-D treatment planning: V. A Fast 3-D photon calculation model. In: *Proceedings of the Ninth International Conference on the Use of Computers in Radiation Therapy*. Amsterdam: North-Holland; 1987. p. 521–5.
- [20] Galvin JM, Xiao Y, Michalski D, et al. Treating oropharyngeal cancer with an inverse planning method that starts from the definition of field segments. In: *43rd Annual ASTRO Meeting*. *Int J Radiat Oncol Biol Phys*, 51.; 2001. p. 76–7.
- [21] Intensity Modulated Radiation Therapy Collaborative Working Group. Intensity-modulated radiotherapy: current status and issues of interest. *Int J Radiat Oncol Biol Phys* 2001;51:880–914.
- [22] Jeraj R, Keall PJ, Siebers JV. The effect of dose calculation accuracy on inverse treatment planning. *Phys Med Biol* 2002;47:391–407.
- [23] Keller-Reichenbecher MA, Bortfeld T, Levegrün S, Stein J, Preiser K, Schlegel W. Intensity modulation with the ‘step and shoot’ technique using a commercial MLC: a planning study. *Int J Radiat Oncol Biol Phys* 1999;45:1315–24.
- [24] Laub W, Alber M, Birkner M, Nüsslin F. Monte Carlo dose computation for IMRT optimization. *Phys Med Biol* 2000;45:1741–54.
- [25] Lee N, Xia P, Quivey JM, et al. Intensity-modulated radiotherapy in the treatment of nasopharyngeal carcinoma: an update of the UCSF experience. *Int J Radiat Oncol Biol Phys* 2002;53:12–22.
- [26] McShan DL, Fraass BA. Use of an octree-like geometry for 3D dose calculations. *Med Phys* 1993;20:1219–27.
- [27] Meedt G, Alber M, Nüsslin F. A method for 3D beam direction optimisation in IMRT. In: *Sixth ESTRO Meeting on Physics for Clinical Radiotherapy*. *Radiother Oncol*; 2001. p. S64–5.
- [28] Roesink JM, Moerland MA, Battermann JJ, Hordijk GJ, Terhaard CHJ. Quantitative dose-volume response analysis of changes in parotid gland function after radiotherapy in the head-and-neck region. *Int J Radiat Oncol Biol Phys* 2001;51:938–46.
- [29] Schwarz M, Bos LJ, Mijnheer BJ, Lebesque JV, Damen EMF. Importance of accurate dose calculations outside segment edges in intensity modulated radiotherapy treatment planning. *Radiother Oncol*, accepted for publication.
- [30] Seco J, Evans PM, Webb S. An optimization algorithm that incorporates IMRT delivery constraints. *Phys Med Biol* 2002;47: 899–915.
- [31] Stein J, Mohan R, Wang XH, et al. Number and orientations of beams in intensity-modulated radiation treatments. *Med Phys* 1997;24: 149–60.
- [32] Sultanem K, Shu HK, Xia P, et al. Three-dimensional intensity-modulated radiotherapy in the treatment of nasopharyngeal carcinoma: the University of California–San Francisco experience. *Int J Radiat Oncol Biol Phys* 2000;48:711–22.
- [33] Wu Q, Manning M, Schmidt-Ullrich R, Mohan R. The potential for sparing of parotids and escalation of biologically effective dose with intensity-modulated radiation treatments of head and neck cancers: a treatment design study. *Int J Radiat Oncol Biol Phys* 2000;46: 195–205.
- [34] Xia P, Fu KK, Wong GW, Akazawa C, Verhey LJ. Comparison of treatment plans involving intensity-modulated radiotherapy for nasopharyngeal carcinoma. *Int J Radiat Oncol Biol Phys* 2000;48: 329–37.